Interactions of Small Molecules and Au Nanoparticles with Solubilized Single-Wall Carbon Nanotubes

Jian Zhang,[†] Gangli Wang,[†] Young-Seok Shon,[†,‡] Otto Zhou,[§] Richard Superfine,[§] and Royce W. Murray*,[†]

Kenan Laboratories of Chemistry and Department of Physics and Astronomy, University of North Carolina, Chapel Hill, North Carolina 27599

Received: October 24, 2002; In Final Form: February 12, 2003

Oxidatively end-cut single-wall carbon nanotube (SWNT) has been solubilized (**sol-SWNT**) in organic solvents by refluxing in aniline and purified by silica gel chromatography. NMR analysis of **sol-SWNT** indicates that the ratio of nanotube carbons to aniline sites is 360:1. A hydroxy-stilbene fluorophore (*trans*-4-nitro-4′-hydroxy stilbene, **1**) adsorbs onto **sol-SWNT**, but can also be demonstrably ester-coupled to the nanotube material, based on comparisons of absorbance spectra. In the combinations of **1** and **sol-SWNT** made by ester-coupling and adsorption, the fluorescences of hydroxy-stilbene and of **sol-SWNT** could be excited selectively and separately. When exciting (500 nm) the **sol-SWNT** in the presence of adsorbed hydroxy-stilbene, the nanotube's emission intensity decreases, but the energetics are unchanged, whereas ester-coupled hydroxy-stilbene diminishes both the **sol-SWNT** energy and intensity. When exciting either adsorbed (at 372 nm) or ester-coupled stilbene (at 347 nm), the stilbene emission intensities are substantially reduced, and a weak, photosensitized **sol-SWNT** emission could be seen. Energy transfer quenching of the stilbene by the nanotube structure produces some quantity of excited states that relax by emission. Mixed monolayer-protected Au clusters adsorb strongly onto both end-opened SWNT and **sol-SWNT**. Adsorption of MPCs with hydroxyl groupings in the mixed monolayer onto end-opened SWNTs occurred without change in shape of the nanotube bundles but could effect the rolling up of the more flexible **sol-SWNT**s. Amine-labeled MPCs were less aggressive adsorbers and the 15−20 nm nanotube bundles of **sol-SWNT** could be imaged, outlined with the adsorbed nanoparticles.

Introduction

Carbon nanotubes have attracted considerable research attention since their introduction in the 1990s. Single-wall carbon nanotubes (SWNTs) have interesting chemical and physical properties,[1−5] and for chemists they offer interesting challenges for functionalization with other chemical entities and combining into useful nanostructures.[6,7] A problem in functionalizing SWNT is the persistent van der Waals aggregation of individual nanotubes into nanotube bundles that are poorly soluble in organic solvents.[8] Dispersing bundles and increasing SWNT solubility in organic solvents is a significant issue, in which there has been progress by attaching solubilizing moieties to the ends of nanotubes,[7,9−11] and by reducing the nanotube lengths and oxidatively opening the nanotube ends ("end-opening") with oxidants such as H_2SO_4/HNO_3.[8] A recent contribution by Wilson et al.[12a] was reaction and dispersal of SWNT bundles by refluxing in aniline. The product, an aniline-derivatized SWNT, is quite soluble in organic solvents.[12a] Other solubilizing procedures have also been reported.[12b,c]

Here, we combine the oxidative[8] "end-opening" of SWNT and the anilination reaction of Wilson et al.[12a] to prepare solubilized SWNT (abbreviated **sol-SWNT**) that can be chromatographically purified of excess and weakly side-wall-adsorbed aniline. Several experiments have been conducted to advance the existing characterization of this material. The solubilized SWNTs are examined spectroscopically and the attachment of small molecules and metal nanoparticles to them is investigated. The small molecule probe is the fluorophore *trans*-4-nitro-4′-hydroxy stilbene (**1**). Stilbene derivatives are known to be quite sensitive to their molecular environment both in solution and in solid state.[13−15] The stilbene derivative **1** adsorbs onto the **sol-SWNT**. We are also able to spectroscopically show that use of an ester-coupling reagent yields a different product in which **1** has been covalently linked to **sol-SWNT**. Interactions of metal nanoparticles with the surfaces of bulk nanotube[16] bundles and with C60 fullerene[17] have been described. Because nanoparticles, in particular the monolayer-protected cluster (MPC) variety, can be flexibly functionalized,[18−20] it would appear that attaching MPCs to solubilized SWNTs offers avenues to combining a wide range of chemical systems with the **sol-SWNT**s. Their strong adsorptive interactions overwhelm, however, observations of covalent nanoparticle-**sol-SWNT** linking. We describe the adsorptive interactions of **sol-SWNT**s with MPCs bearing mixed monolayers of hexanethiolate (C6) and ω-hydroxyhexanethiolate (HOC6), ω-hydroxybutanethiolate (HOC4), or ω-aminehexanethiolate (NH_2C6). The mixed monolayer MPCs were prepared from C6 MPCs using place exchange reactions,[18] and the adsorption was detected by transmission electron microscopy (TEM).

Experimental Section

Chemicals. All reagents (Aldrich), spectroscopic grade solvents (Fisher, Aldrich), and deuterated solvents (Isotech,

[†] Kenan Laboratories of Chemistry.

[‡] Present address: Department of Chemistry, Western Kentucky University, 1 Big Red Way, Bowling Green, KY 42101.

[§] Department of Physics and Astronomy.

10.1021/jp0273068 CCC: $25.00
Published on Web 03/28/2003

SCHEME 1: Acylation of Compound 1.

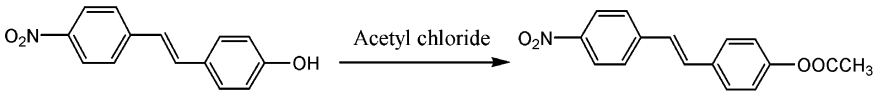

Compound **1** Compound **2**

SCHEME 2: Preparation of Functionalized MPCs.

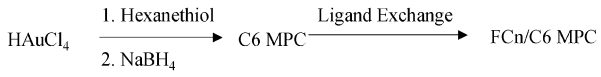

n: 4 and 6, F: -NH_2 or -OH

Aldrich) were used as received. Single-wall carbon nanotubes were purchased from Carbon Nanotechnologies, Inc. (Rice University). Reactions were monitored by thin-layer chromatography on 0.25 mm Merck silica gel plates (60F-254), while Baxter silica gel 60 Å (230−400 mesh ASTM) was used for flash column chromatography.

Stilbene Synthesis. *trans*-4-Nitro-4′-hydroxy stilbene (compound **1**)[21] was prepared as previously described. *trans*-4-Nitro-4′-acetylhydroxy stilbene (compound **2**) was obtained by condensation of compound **1** with acetyl chloride in CH_2Cl_2 (Scheme 1).

Solubilized SWNT (sol-SWNT). The SWNT were incubated in a 3:1 mixture of concentrated sulfuric and nitric acids for 40 min; after this oxidative procedure the nanotubes are shortened and their end openings should bear oxidized carbon sites such as carboxylic acids.[8] This product was collected on a Millipore porous filter (FHLC04700, 0.45 μm) after diluting 20 times with water. Then 40 mg of the thusly end-opened SWNT was refluxed in 5 mL of aniline in the dark for 4 h,[12a] after which the reaction mixture was flash chromatographed on a silica gel column. After the SWNT reaction mixture was added to the column, it was first flushed with CH_2Cl_2 to remove excess aniline and side products, and then with CH_2Cl_2/methanol (4:1) to elute the purple colored band of solubilized nanotubes (**sol-SWNT**) in a yield of 32 mg.

Sol-SWNT-Stilbene Derivative and Adsorptive Adduct. The sol-SWNT-stilbene derivative **3** was prepared by stirring a solution of 10 mg of **sol-SWNT**, 30 mg of the condensation reagent 1,3-dicyclohexylcarbodiimide (DCC), and 30 mg of *trans*-4-nitro-4′-hydroxystilbene (**1**) in 30 mL of THF at room temperature for 12 h. The solvent was removed under vacuum and the residue placed on a silica gel column, which was flushed with CH_2Cl_2 until no excess of compound **1** could be detected (stilbene fluorescence) in the eluent. Then (4:1) CH_2Cl_2/methanol was added to the column to elute **3** (a purple band). The sol-SWNT-stilbene adsorptive adduct (**4**) was obtained by an analogous procedure in which the DCC ester-coupling reagent was omitted.

Hexanethiolate-Coated and Mixed Monolayer MPCs. The hexanethiolate-coated nanoparticles (C6MPCs) were prepared using the Brust reaction[18,22] with a 2:1 molar ratio of hexanethiol and $HAuCl_4$ in toluene. In previous work[20c] this condition gave MPCs with an average core size of Au_{225} and an average 71 number of ligands. The Au(I) thiolate complex was reduced at 0 °C with a 10-fold excess of $NaBH_4$ added as an aqueous solution, after which the reaction mixture was stirred for 24 h at room temperature. The MPCs were recovered by removing the water layer, evaporating the toluene, followed by thorough washing with ethanol. The mixed monolayer MPCs were obtained by stirring THF solutions containing 1:3 mole ratios of functionalized thiol:hexanethiolate/MPC for 72 h at room temperature. The functionalized thiols were ω-hydroxybutanethiol, ω-hydroxyhexanethiol, and ω-aminohexanethiol. The compound 6-amino-1-hexanethiol was prepared as previously described.[23] The products were precipitated and washed with 1:1 methanol/acetonitrile. The mixed monolayer compositions were assessed by ^{1}H NMR spectra of the disulfides quantitatively liberated from the MPCs upon their decomposition with iodine;[19a] the results were (average composition) $Au_{225}(C6)_{51}(C6OH)_{20}$, $Au_{225}(C6)_{54}(C4OH)_{17}$, and $Au_{225}(C6)_{57}(C6NH_2)_{14}$. Larger hexanethiolate-coated nanoparticles,[20c] prepared using a mole ratio of 1:10 of hexanethiol and $HAuCl_4$, and functionalized with 6-amino-1-hexanethiol by a ligand-exchanged reaction as analogous methods of small-size MPCs. The result was (average composition) $Au_{4023}(C6)_{265}(C6NH_2)_{188}$.

SWNT-MPC Adsorptive Adducts. Equal volumes of THF solutions of mixed monolayer MPCs (1 mg/mL) and either end-opened SWNT or **sol-SWNT** (1 mg/mL) were combined. In the case of MPCs with mixed monolayers of hexanethiolate and ω-hydroxyhexanethiolate (or ω-hydroxybutanethiolate), a precipitate formed when these solutions were mixed. Precipitation did not occur for mixed monolayer hexanethiolate/ω-aminohexanethiolate MPC solution mixtures with **sol-SWNT**, which were stirred for 72 h; the solvent was removed under vacuum and the residue chromatographed on silica gel, recovering the sol-SWNT-MPC adsorptive adduct band by elution with 4:1 CH_2Cl_2/methanol.

Spectra. ^{1}H NMR spectra were recorded on Varian UNITY plus-300 spectrometer; transmission FTIR spectra of sample films cast on a KBr plate were measured with a Bio-RAD FTS 6000 FT-IR spectrometer. Absorption and fluorescence spectra were recorded with Unicam UN4 spectrophotometer and Spex Fluoro-log spectrofluorometer in 1 cm quartz cells, respectively. Transmission electron micrographs (TEM) were taken with a side-entry Phillips CM12 electron microscope operated at 120 kev. Samples were cast from methylene chloride solutions onto standard carbon-coated (200−300 Å) Formvar films on copper grids (400 mesh).

Results and Discussion

***trans*-4-Nitro-4′-hydroxy Stilbene (1) and Its Acylated Derivative (2).** Stilbene spectra are sensitive to changes of functional groupings. The acylated derivative of **1** was prepared (Scheme 1, compound **2**) in order to exploit the difference between the absorbance and emission spectra of **1** vs **2** as evidence for formation of an ester bond between **1** and **sol-SWNT**. Figure 1 shows that **1** exhibits an absorbance maximum at 378 nm in CH_2Cl_2, and when excited at that wavelength, exhibits a fluorescence emission maximum at 548 nm. The acylated derivative **2** absorbs at 354 nm and emits at 522 nm when excited at 354 nm. Compounds **1** and **2** have, at the same concentrations, similar absorbances and emission intensities as shown in the figure. The key aspect of Figure 1 is that the absorbance and emission maxima of **2** differ perceptibly from those of **1**, being both shifted by >20 nm to higher energy.

Sol-SWNT. The oxidative end-opening and aniline reaction of SWNT bundles (see Experimental Section) produced a deep

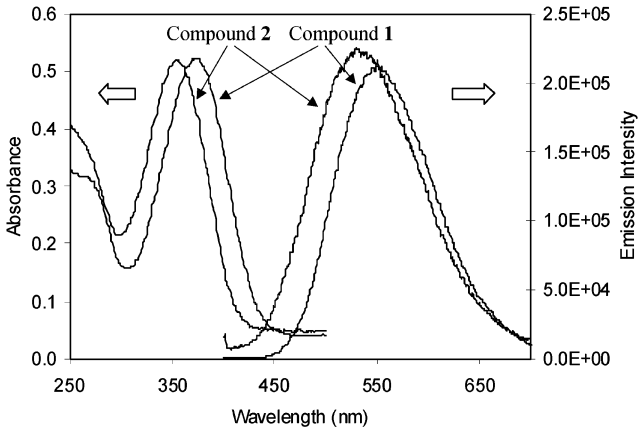

Figure 1. Absorbance and emission spectra of compounds **1** and **2** (1.2×10^{-5} M) in CH_2Cl_2. The fluorescence spectra of **1** and **2** are excited at their respective absorption maxima (378 and 354 nm). The fluorescence maxima of **1** and **2** lie at 548 and 522 nm, respectively.

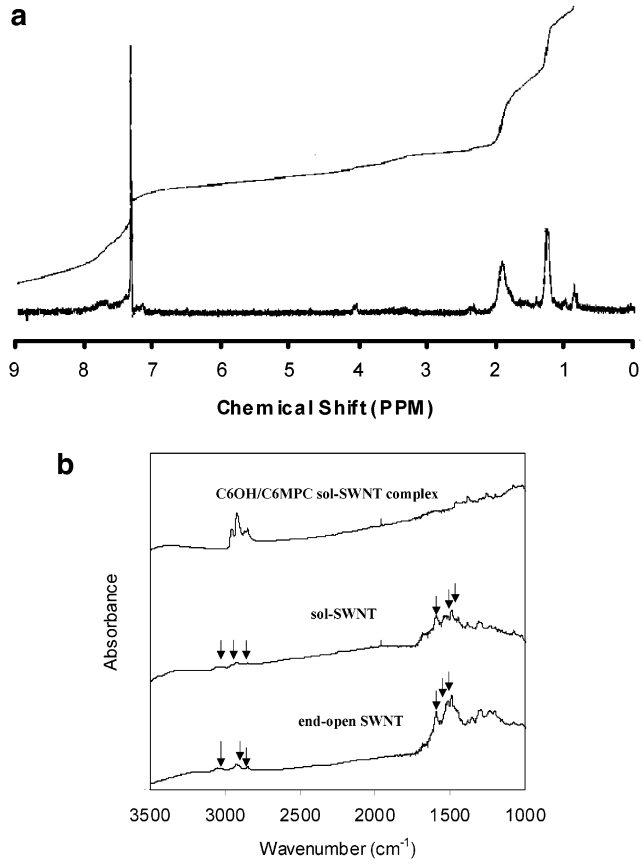

Figure 2. (a) ^{1}H NMR spectroscopy of **sol-SWNT** in $CDCl_3$. (b) FTIR spectra of end-opened SWNT, of **sol-SWNT**, and of C6OH/C6MPC-sol-SWNT adsorption/aggregate.

purple solution in the aniline reaction mixture. The proposed mechanism of dissolution involves the addition of aniline onto unsaturated C═C bonds of the SWNT, accompanied by exfoliation of the SWNT bundles into individual nanotubes or bundles containing significantly smaller numbers of SWNTs.[12a] We found that the solubilized SWNTs could be purified of excess and weakly adsorbed aniline by simple flash chromatography on silica gel. The **sol-SWNT** product is soluble in methylene chloride, acetone, alcohol, and tetrahydrofuran, and slightly soluble in toluene; the solutions are purple in color.

Figure 2a shows a ^{1}H NMR spectrum of sol-SWNT. The weak and broadened multiplet at 7.0−8.0 ppm can be attributed to aniline aromatic protons, either from the aniline functionalization or from residual, strongly adsorbed aniline. These peaks, relative to those at lower chemical shift, are enhanced by longer refluxing times of aniline+SWNT mixtures, implying that the quantity of aniline derivatization increases with reaction time. The sharp peak at 7.24 ppm is due to $CHCl_3$ impurity in the deuterated solvent. Other, more intense proton resonances are seen at 0.9, 1.2, and 1.9 ppm. According to their chemical shifts, these peaks are inconsistent with the solvents (CH_2Cl_2 and methanol) used in the chromatographic isolation and with other impurities, such as acetone, water, or SWNT terminal COOH groups. The chemical shifts and the broadening of these high field peaks lead us to assign them to alkylic proton sites on the SWNT structure. The anilination reaction should produce a single alkylic proton per aniline.[12a] That the area under the high field peaks is more than that under the aniline peak implies that a considerable quantity of other alkylic protons exist on the **sol-SWNT**. Such chemistry represents a little understood aspect of these carbon materials. Finally, we note that the broadening of the NMR peaks is consistent with the large dimension (and slow rotational diffusion) of the **sol-SWNT** entity.

The aniline NMR peak allows a rough assessment of the extent of anilination of **sol-SWNT**. In a solution of 14 mg of sol-SWNT and 0.03% TMS (v/v) in 1.1 mL of CD_2Cl_2 the concentration of aniline was estimated from the ratio of aniline and TMS protons to be 4.1×10^{-3} M, giving a mole ratio of nanotube carbons/aniline of ca. 360:1. The chemical modification of only a small portion of the nanotube C═C bonds thus greatly alters the SWNT solubility. From the high field peaks, the mole ratio of nanotube carbon/alkylic proton on **sol-SWNT** is ca. 17:1, implying that ca. 6% of the nanotube carbon atoms bear alkylic hydrogen.

Proton sites on end-opened SWNT and **sol-SWNT** were confirmed (Figure 2b) by the three weak C−H stretch bands seen in FTIR spectroscopy of SWNT at 3076 cm^{-1} (aromatic), and 2982 and 2875 cm^{-1} (alkylic). For **sol-SWNT** these peaks appear at 3084, 2982, and 2875 cm^{-1}, respectively. The obvious implication is that the proton sites preexist before anilination. There are for SWNT more peaks at 1700 cm^{-1} (possibly C═O stretch mode of carboxylic acid) and at 1596, 1523, and 1497 cm^{-1} (possibly C═C stretch modes of the carbon nanotube), which are relatively unchanged in the FTIR spectrum of **sol-SWNT**.

The UV−vis spectrum of **sol-SWNT** displays absorbance maxima at 290 and 532 nm (Figure 3, lower curve). The very broad lower energy band has been[12a] speculated to be a charge transfer between aniline and SWNT. The higher energy band position is typical of small aromatic systems, and in fact is near the 280 nm aniline band. When **sol-SWNT** is excited at 500 nm, its fluorescence (Figure 4, upper curve) exhibits peaks at 562 and 610 nm, analogous to those reported previously.[12]

Sol-SWNT-Stilbene Derivative 3 and Adsorptive Adduct 4. These two products of treating **sol-SWNT**s with stilbene in the presence and absence, respectively, of a coupling reagent are both soluble in organic solvents, and they exhibit ^{1}H NMR and FTIR spectra that are similar to those of **sol-SWNT**. Presumably the amount of attached stilbene is too small to be detected relative to the responses of the **sol-SWNT** itself.

The absorption spectrum of the **sol-SWNT**-stilbene derivative **3** is markedly different from that of **sol-SWNT**, having the lower energy band blue shifted to 480 nm (the nanotube is less electron-accepting) and a more intense peak at 285 nm. In contrast, the spectrum of the absorptive adduct **4** (Figure 3) is

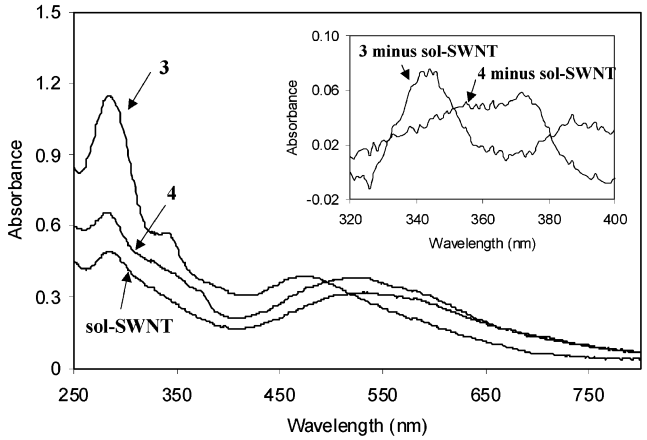

Figure 3. Absorbance spectra of **sol-SWNT**, ester-coupled combination of **1** and **sol-SWNT** (**3**) (0.1 mg/mL), and adsorption-based combination of **1** and **sol-SWNT** (**4**) (0.1 mg/mL) in CH_2Cl_2. The absorbance bands in the difference spectra in the insert indicate ca. 1.4×10^{-6} mol of stilbene present per 0.1 mg of nanotube.

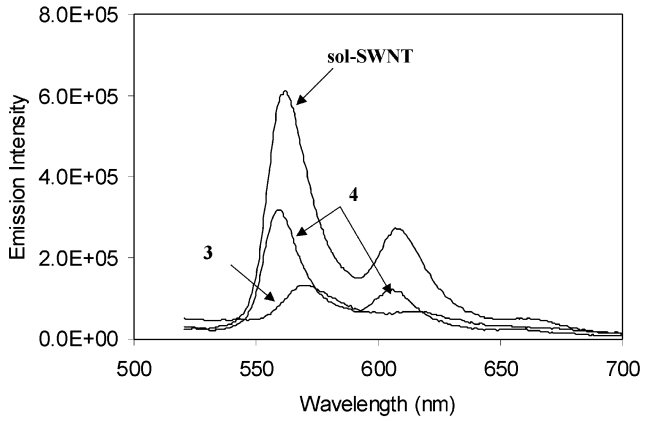

Figure 4. Fluorescence spectra of **sol-SWNT**, ester-coupled combination of **1** and **sol-SWNT** (**3**) (0.1 mg/mL), and adsorption-based combination of **1** and **sol-SWNT** (**4**) (0.1 mg/mL) in CH_2Cl_2 when photoexcited at 500 nm.

quite similar to that of **sol-SWNT**, showing band maxima at 288 and 532 nm. In both **3** and **4** there appear small shoulders in the 320−400 nm range; by comparison to Figure 1 these arise from stilbene and are important features in that they signal ester-coupling and adsorptive attachment to the **sol-SWNT**. Taking difference spectra of **3** and **sol**-SWNT, and of **4** and **sol-SWNT,** gives the spectra in the inset of Figure 3. The difference spectrum of **3** from **sol-SWNT** shows a clear maximum at 347 nm, which is close to the 354 nm seen for compound **2** in Figure 1 and can be taken as evidence for ester bond formation between the stilbene **1** and carboxylic acid groupings on **sol-SWNT**. Presumably the coupling reaction product **3** lies at the **sol-SWNT** ends although we have no direct evidence for this. From the relative absorbances of **2** in Figure 1 and of **3** in Figure 3, inset, one can estimate that the band in Figure 3, inset, represents ca. 1.4×10^{-5} mol of stilbene attached per gram of **sol-SWNT,** which translates to a mole ratio of nanotube carbons:stilbene of 10^4:1. According to this mole ratio, the length of SWNT would be 2.4 μm assuming that a single stilbene is coupled at the nanotube ends and that the thickness of the unit structure is 0.24 nm.[24] This length is obviously shorter than the real value (mostly longer than 10 μm, see Figure 6d), meaning that multiple stilbene molecules are end-coupled, and/or some are side-coupled to defects on the SWNT side wall, generated by the oxidative short-cut procedure. The more poorly

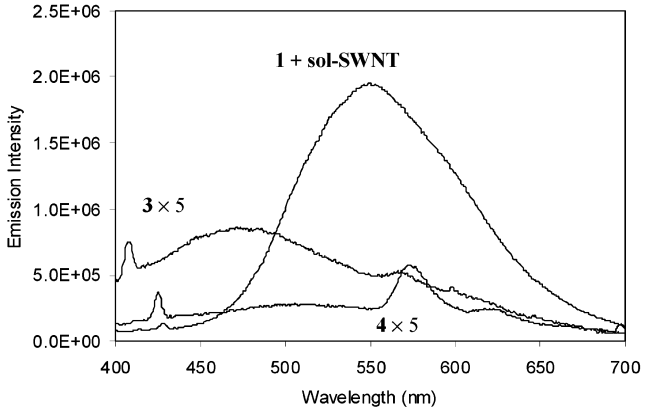

Figure 5. Fluorescence spectra of **1** + **sol-SWNT** (a solution containing codissolved **1** 1.4×10^{-6} M and **sol-SWNT** 0.1 mg/mL, excited at 372 nm), of **3** (0.1 mg/mL, excited at 372 nm), in CH_2Cl_2, and of **4** (0.1 mg/mL, excited at 347 nm). Spectra for **3** and **4** are at 5× higher sensitivity. Spectra of **3** and **4** each correspond to equal amounts (ca. 1.4×10^{-6} mol) of stilbene present.

defined difference spectrum between the adsorptive adduct **4** and **sol-SWNT** in Figure 3, inset, indicates a roughly similar quantity of adsorbed stilbene. The 372 nm band is close to that of the stilbene compound **1** (378 nm) in Figure 1. This band apparently arises from stilbene that (in the absence of the DCC coupling reaction environment) becomes strongly adsorbed on the **sol-SWNT** side walls. It is unclear why this adsorption does not occur concurrently with stilbene derivatization of **sol-SWNT** (i.e., **3**) unless adsorption of the DCC coupling reagent displaces otherwise adsorbed stilbene. The speculation that **sol-SWNT**-stilbene adsorptive adduct **4** is actually confined *inside* the SWNT structure, which is prevented in **3** because of blocking by end-coupled stilbene, is considered possible but less plausible.

The **sol-SWNT**-stilbene adsorptive adduct **4** displays fluorescence (Figure 4) analogous to that of **sol-SWNT**, with bands at 560 and 606 nm (when excited at 500 nm), but with a lowered emission intensity. (The solutions contain equal masses of **sol-SWNT**, **3**, and **4**.) Note that excitation at 500 nm *selectively* excites the **sol-SWNT** luminescence; according to Figure 1, **1** and **2** have negligible absorption at 500 nm. Additionally, the **sol-SWNT** emission peaks are notably sharper than those of the stilbenes (Figure 1). The fluorescence from **sol-SWNT**-stilbene derivative **3** is, on the other hand, clearly red-shifted to 571 nm with a shoulder at 620 nm, and has a substantially weakened emission intensity. These results show that the consequences of stilbene adsorption and coupling to **sol-SWNT** are qualitatively different, which is consistent with the absorption spectra of Figure 3, inset. The results further show that the luminescence of **sol-SWNT** is seriously altered by the ester-coupling of stilbene to the nanotube ends and side-wall defects (assuming that is where coupling actually occurs). This intriguing result, suggests, consistent with a previous observation,[9a] that whatever the origin of **sol-SWNT** luminescence is, the *electronic states associated with it may be localized* on the nanotube structure near or on the **sol-SWNT** ends and side-wall defects.

When compound **1** is simply codissolved with **sol-SWNT** in CH_2Cl_2, and the stilbene is excited at 370 nm (a wavelength appropriate for exciting **1**, Figure 1), an intense fluorescence peak occurs at 552 nm (Figure 5) that is near the fluorescence maximum (548 nm) of **1,** and has a similar spectral shape. The Figure 5 spectrum was taken within minutes after codissolution so as to minimize the extent of adsorptive interaction of **1** with **sol-SWNT**. Excitation at 350−370 nm of a solution containing

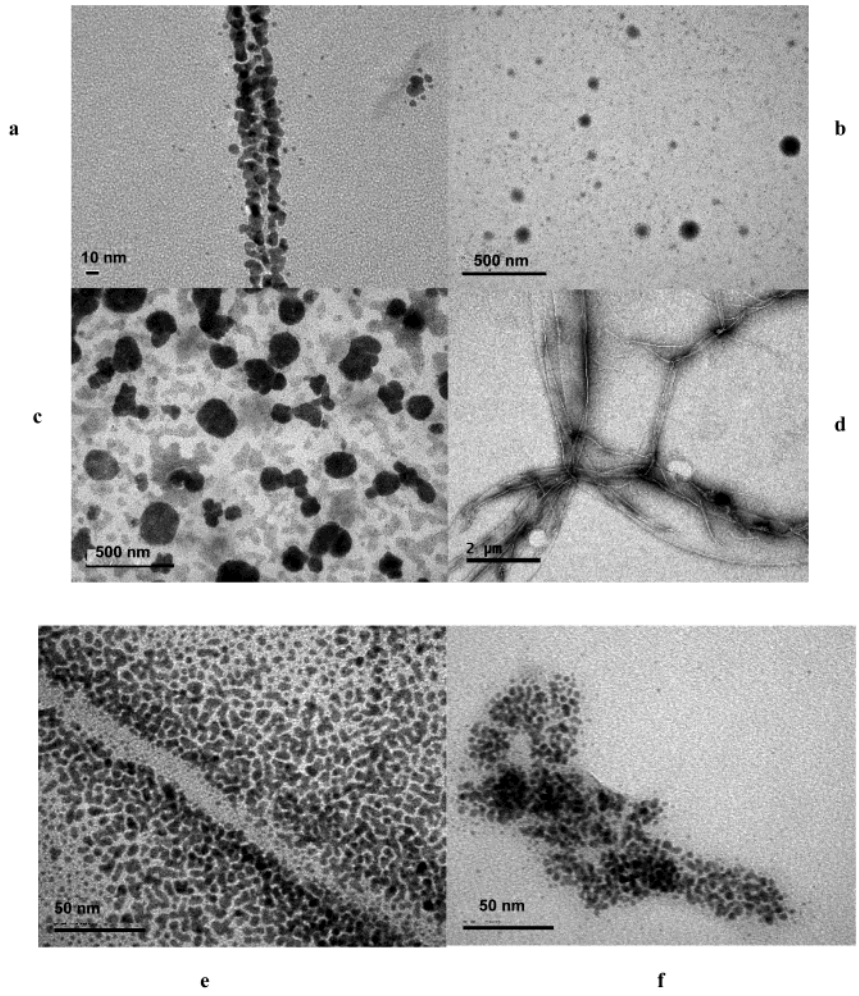

Figure 6. Transmission electron micrographs (TEM) of (a) C6OH/C6MPC adsorbed on end-opened SWNT (the bar is 10 nm), (b) C6OH/C6MPC adsorbed on**sol-SWNT**, (c) C4OH/C6MPC adsorbed on **sol-SWNT**, (d) $C6NH_2$/C6MPC adsorbed on **sol-SWNT**, (e) an enlargement of a portion of (d), and (f) larger $C6NH_2$/C6MPC adsorbed on **sol-SWNT**.

only **sol-SWNT** produces no emission. The intense emission of the solution of **1** and **sol-SWNT** in Figure 5 can be attributed completely to compound **1**.

In contrast, excitation of the **sol-SWNT**-stilbene derivative **3** at 372 nm produces (Figure 5) a broad, weak, blue-shifted emission with a maximum at 482 nm that probably arises from stilbene moieties coupled to **sol-SWNT**. Additionally, there are weak but narrow emission peaks at ca. 570 nm with a shoulder at 610 nm, which probably arise from the **sol-SWNT** itself. Figure 5 also shows the 372 nanometer-excited narrow-band fluorescence from **4** at 577 nm with a shoulder at 625 nm that can be attributed to the **sol-SWNT.** There is only a hint of a band at ca. 510 nm for the adsorbed stilbene in **4**.

The results in Figure 5 are interesting in three important regards. First, the stilbene luminescence is substantially quenched (relative to free stilbene) by both ester coupling and adsorption onto **sol-SWNT**. This quenching probably occurs by efficient energy transfer from stilbene into the **sol-SWNT** electronic manifold. Second, observing **sol-SWNT** luminescence from **3** and **4**, however weakly, signals that, when excited at 372 nm, *energy transfer* from the ester-coupled or adsorbed stilbene moiety can act as a sensitizer[14] of **sol-SWNT** emission. Photosensitization of SWNTs has to our knowledge not been previously reported, but is well-known in molecular chemistry. Third, even though the absorbance spectra of the stilbene ester **2** (Figure 1) and of the **sol-SWNT**-stilbene derivative **3** (Figure 3, inset) are similar, the fluorescence of stilbene that is ester-coupled to **sol-SWNT** (i.e., in **3**) occurs at higher energy (Figure 5) than that of **2** (Figure 1). That is, the emission manifold of the stilbene in **3** has been altered by its attachment to the **sol-SWNT**, in a manner favoring emission from higher energy states.

SWNT-MPC. The hexanethiolate MPC had an *average* composition $Au_{225}(C6)_{71}$ with 2.0 nm diameter prior to place exchange.[20c] To make the mixed monolayer MPCs, hexanethiolate ligands were place exchanged in reactions with 4-mercapto-1-butanol, 6-mercapto-1-hexanol, and 6-mercapto-1-hexaamine. We label the products C6OH/C6 MPC, C4OH/C6 MPC, and $C6NH_2$/C6 MPC, respectively. The resulting mixed monolayer shells, as determined by ^1H NMR, have average numbers of ligands, respectively, of $Au_{225}(C6)_{51}(C6OH)_{20}$, $Au_{225}(C6)_{54}(C4OH)_{17}$, and $Au_{225}(C6)_{57}(C6NH_2)_{14}$.

When end-opened SWNT were dispersed in a THF solution of C6OH/C6 MPC, the absorption spectrum of the nanoparticle gradually decreased with time, reflecting adsorptive attachment of MPCs onto the SWNT surface and ensuing precipitation. Figure 6a shows a transmission electron micrograph of the end-opened-SWNT-MPC adsorptive adduct. It is clear from the image that the MPCs have adsorbed all along the length of the SWNTs and in the example shown serve to outline two collinear bundles of nanotubes.

The results of exposing MPCs in solutions to codissolved **sol-SWNT** varied sharply with the exterior chemical functionality of the MPC. Mixing THF solutions of **sol-SWNT** with MPCs

with mixed C6OH/C6 monolayers resulted in precipitation of solid material that could not be redissolved in organic solvents. Use of mixed monolayer C4OH/C6 MPCs (the idea was to slightly recess the hydroxyl functions within the monolayer) produced the same result. The TEM images of these adsorptive products (Figure 6b,c, respectively) show large, crudely spherical objects and no isolated **sol-SWNT** strands, very unlike those of end-opened-SWNT adsorptive adducts (Figure 6a). We propose that the spherical images in Figures 6b,c represent **sol-SWNT**s that have formed aggregate mixtures of nanotubes and nanoparticles in which the nanotubes have been "rolled up" to a very considerable degree, and their solubility is lost. The effect may be a combination of the polyhydroxylated MPCs adsorbed on **sol-SWNT** acting as cross-linkers between nanotube side walls, and a considerably lowered stiffness of the anilinated, solubilized **sol-SWNT**s. The end-opened SWNTs apparently retain enough stiffness and rigidity to resist "rolling-up" aggregation even though the adsorptive interactions may be just as strong.

Effects intermediate to those in Figures 6a−c were observed when amine-functionalized MPC and **sol-SWNT** solutions are mixed. In this case, precipitation did not occur and the images of Figures 6d−f were obtained. Figure 6d shows that the nanotubes remain in an extended form, with MPCs adsorbed along the side walls. In one image (Figure 6e), the adsorption (or aggregation during drying) served to outline the **sol-SWNT** image, which has an apparent average width of ca. 15 nm. This sample of **sol-SWNT** retains the common nanotube bundling, but the bundle width is much smaller than that of as-received SWNTs, consistent with the anilination serving to exfoliate (to some extent) the as-received bundle of nanotubes. Figure 6d also shows high populations of MPCs where the **sol-SWNTs** (or bundles of) lie close together or cross, implying that like the hydroxylated MPC analogues, the amino MPCs can act as cross-linking agents. In fact, silica gel chromatography will remove adsorbed C6NH2/C6 MPCs from **sol-SWNT**, as confirmed by the absence of MPCs in TEM images of the product. (The adsorptive adducts between **sol-SWNT** and hydroxylated MPCs, in contrast, could not be chromatographically separated.) Figure 6f shows another experiment with somewhat larger amine-functionalized MPCs, where the adsorptive-adduct nanotubes again seem to be partially "rolled-up", but in this case could not be chromatographically separated from the MPCs. The 30 nm roughly spherical images in Figure 6f are smaller than those in Figures 6b,c, and in this case the adsorptive adducts remained soluble in organic solvents. The adsorption of MPCs onto **sol-SWNT** can thus produce a variety of topological and chemical effects.

The FTIR spectrum (Figure 2b) of the **sol-SWNT** C6OH/C6 MPC adsorptive adduct displays C−H stretch bands at 2961, 2924, and 2873 cm^{-1}, and weak bands at 1630, 1469, and 1265 cm^{-1} that may arise from N−H (residual aniline), C−H, and C−O wagging, respectively. The strong C−H stretch bands are consistent with the incorporation of a considerable quantity of MPCs and their methylene chains into the precipitated aggregate formed with the **sol-**SWNT material.

Conclusions

In this paper, we have solubilized end-opened single-wall carbon nanotubes by reaction with aniline and purified them with flash chromatography. This material, **sol-SWNT**, consists of partly exfoliated nanotube bundles (Figure 6d) of ca. 15 nm diameter, and bears anilinated sites in a proportion of ca. 360:1 nanotube carbons per aniline. Apparently only a small degree of anilination can greatly improve the nanotube solubility. A hydroxy-stilbene fluorophore **1** adsorbs onto **sol-SWNT**, but can also be demonstrably ester-coupled to the nanotube material, based on comparisons of absorbance spectra (Figures 1 and 3). There were a number of interesting effects on the fluorescence properties of combinations of **1** and **sol-SWNT** made by ester coupling (**3**) and adsorption (**4**). The fluorescence of **1** and of **sol-SWNT** could be excited selectively and separately. When selectively exciting (500 nm) the **sol-SWNT,** adsorbed **1** causes a diminution of the nanotube's emission intensity, but not its energetics. On the other hand, ester-coupled **1** changed the **sol-SWNT** emission to lower energies as well as diminishing it. When selectively exciting (372 nm) either adsorbed or ester-coupled stilbene **1**, the stilbene emission intensities are substantially reduced, but a weak, photosensitized **sol-SWNT** emission could be seen. This makes it evident that energy transfer quenching of the stilbene by the nanotube structure produces some quantity of excited states that relax by emission. Whether this sensitized emission has any directionality relative to the axis of the nanotubes emitter is an interesting and potentially important question.

In the case of the monolayer-protected Au clusters, only adsorptive interactions with the nanotubes were described. TEM images showed that MPCs with mixed C6OH/C6 monolayers adsorb strongly onto the side walls of end-opened SWNTs, which retain their rigid linear shapes. Adsorption of hydroxy-labeled MPCs onto **sol-SWNT**s on the other hand appeared to roll these more flexible nanotubes up into spherical nanoparticle/nanotube aggregates, probably by cross-linking aspects of the adsorption. Amino-labeled MPCs were less aggressive in that regard, and could be observed to adsorb all over the **sol-SWNT** side walls, outlining the 15−20 nm nanotube bundles for TEM imaging.

Acknowledgment. This research was supported by a MURI grant from (O.Z.) the Office of Naval Research and by the National Science Foundation (R.W.M.).

References and Notes

(1) (a) Iijima, S. *Nature* **1991**, *354*, 56. (b) Calvert, P. *Nature* **1992**, *357*, 365. (c) Yakobson, B. I.; Smalley, R. E. *Am. Sci.* **1997**, *85*, 324. (d) Tans, S. J.; Devoret, M. H.; Dai, H.; Thess, A.; Smalley, R. E.; Geerligs, L. J.; Dekker: C. *Nature* **1997**, *386*, 474. (e) Wong, E. W.; Sheehan, P. E.; Lieber, C. M. *Science* **1997**, *277*, 1971. (f) Calvert, P. *Nature* **1999**, *399*, 210.

(2) (a) Dresselhaus, M S.; Dresselhaus, G.; Eklund, P. C. *Science of Fullerenes and Carbon Nanotubes*; Academic Press: New York, 1996. (b) Ebbesen, T. W. *Carbon Nanotubes: Preparation and Properties*; CRC Press: Boca Raton, FL, 1997.

(3) (a) Dillon, A. C.; Gennet, T.; Jones, K. M.; Alleman, J. L.; Parilla, P. A.; Heben, M. J. *Adv. Mater.* **1999**, *11*, 1354−1358. (b) Paulson, S.; Helser, A.; Buongiorno Nardelli, M.; Taylor, R. M., II; Falvo, M.; Superfine, R.; Washburn, S. *Science* **2000**, *290*, 1742. (c) Falvo, M. R.; Taylor, R. M., II; Helser, A.; Chi, V.; Brooks Jr., F. P.; Washburn, S.; Superfine, R. *Nature* **1999**, *397*, 236. (d) Falvo, M. R.; Clary, G. J.; Taylor, R. M., II; Chi, V.; Brooks, F. P., Jr.; Washburn, S.; Superfine, R. *Nature* **1997**, *389*, 582.

(4) (a) Sun, L.; Crooks,R. M. *J. Am. Chem. Soc.* **2000**, *122*, 12340. (b) Tang, B. Z.; Xu, H. *Macromolecules* **1999**, *32*, 2569.

(5) Ajayan, P. M.; Zhou, O. In *Synthesis, Structure, Properties, and Applications*; Dresselhaus, M. S., Dresselhaus, G., Avouris, P., Eds.; Topics in Applied Physics 80; Springer-Verlag Press: Heidelberg, 2001.

(6) (a) Zhang, Y.; Shi, Z.; Gu, Z.; Iijima, S. *Carbon* **2000**, *38*, 2055. (a) Bahr, J. L.; Yang, J.; Kosynkin, D. V.; Bronikowski, M. J.; Smalley, R. E.; Tour, J. M. *J. Am. Chem. Soc.* **2001**, *123*, 6536. (b) Bahr, J. L.; Tour, J. M. *Chem. Mater.* **2001**, *13*, 3823.

(7) (a) Chen, J.; Hamon, M. A.; Hu, H.; Chen, Y.; Rao, A. M.; Eklund, P C.; Haddon, R. C. *Science* **1998**, *282*, 95. (b) Hamon, M. A.; Chen, J.; Hu, H.; Chen, Y.; Itkis, M.; Rao, A. M.; Eklund, P. C.; Haddon, R. C. *Adv. Mater.* **1999**, *11*, 834. (c) Niyogi, S.; Hu, H.; Hamon, M. A.; Bhowmik, P.; Zhao, B.; Rozenzhak, S. M.; Chen, J.; Itkis, M E.; Meier, M. S.; Haddon,

R. C. *J. Am. Chem. Soc.* **2001**, *123*, 733. (d) Zhao, B.; Hu, H.; Niyogi, S.; Itkis, M. E.; Hamon, M. A.; Bhowmik, P.; Meier, M. S.; Haddon, R. C. *J. Am. Chem. Soc.* **2001**, *123*, 11673.

(8) Liu, J.; Rinzler, A. G.; Dai, H.; Hafner, J. H.; Bradley, R. K.; Boul, P. J.; Lu, A.; Liverson, T.; Shelimov, K.; Huffman, C. B.; Rodriguez-Macias, F.; Shon, Y.-S.; Lee, T. R.; Colbert, D. T.; Smalley, R. E. *Science* **1998**, *280*, 1253.

(9) (a) Riggs, J. E.; Guo, Z.; Carroll, D. L.; Sun, Y. P. *J. Am. Chem. Soc.* **2000**, *122*, 5879. (b) Sun, Y.-P.; Guduru, R.; Lawson, G. E.; Mullins, J. E.; Guo, Z.; Quinlan, J.; Bunker, C. E.; Gord, J. R. *J. Phys. Chem. B*, **2000**, *104*, 4625. (c) Sun, Y. P.; Huang, W. J.; Lin, Y.; Fu, K. F.; Kitaygorodskiy, A.; Riddle, L. A.; Yu, Y. J.; Carroll, D. L. *Chem. Matter*. **2001**, *13*, 2864.

(10) Baran, P. S.; Khan, A. U.; Schuster, D. I.; Wilson, S. R. *Fullerene Sci. Technol*. **1999**, *7*, 921.

(11) (a) Bahr, J. L.; Mickelson, E. T.; Bronikowski, M. J.; Smalley, R. E.; Tour, J. M. *Chem. Commun*. **2001**, *2*, 193. (b) Mickelson, E. T.; Chiang, I. W.; Zimmerman, J. L.; Boul, P. J.; Lozano, J.; Liu, J.; Smalley, R. E.; Hauge, R. H.; Margrave, J. L. *J. Phys. Chem. B* **1999**, *103*, 4318.

(12) (a) Sun, Y.; Wilson, S. R.; Schuster, D. *J. Am. Chem. Soc*. **2001**, *123*, 5348. (b) Bahr, J. L.; Yang, J.; Kosynkin, D. V.; Bronikowski, M. J.; Smalley, R. E.; Tour, J. M. *J. Am. Chem. Soc.* **2001**, *123*, 6536. (c) Georgakilas, V.; Kordatos, K.; Prato, M.; Guldi, D. M.; Holzinger, M.; Hirsch, A. *J. Am. Chem. Soc.* **2002**, *124*, 760.

(13) (a) Turro, N. J. *Modern Molecular Photochemistry*; Benjamin-Cummings Publishing Company: New York, 1978. (b) Murov, S. L.; Carmichael, I.; Hug, G. L. *Handbook of Photochemistry*, 2nd ed.; Marcel Dekker: New York, 1993.

(14) (a) Whitten, D. G.; Chen, L.; Geiger, H. C.; Perlstein, J.; Song X. *J. Phys. Chem. B* **1998**, *102*, 10098. (b) Song X.; Perlstein, J.; Whitten, D. G. *J. Phys. Chem. A* **1998**, *102*, 5440. (c) Song X.; Perlstein, J.; Farahat, M.; Perlstein, J.; Whitten, D. G. *J. Am. Chem. Soc.* **1997**, *119*, 9144.

(15) (a) Zhang, J.; Whitesell, J. K.; Fox, M. A. *Chem. Mater.* **2001**, *13*, 2323. (b) Hu, J.; Zhang, J.; Liu, F.; Kittredge, K.; Whitesell, J. K.; Fox, M. A. *J. Am. Chem. Soc.* **2001**, *123*, 1464.

(16) Fullam, S.; Cottell, D.; Rensmo, H.; Fitzmaurice D. *Adv. Mater*. **2000**, *12*, 1430.

(17) Brust, M.; Kiely, C. J.; Bethell, D.; Schiffrin, D. J. *J. Am. Chem. Soc.* **1998**, *120*, 12367.

(18) Templeton, A. C.; Wuelfing, W. P.; Murray, R. W. *Acc. Chem. Res.* **2000**, *33*, 27.

(19) Ingram, R. S.; Hostetler, M. J.; Murray, R. W. *J. Am. Chem. Soc.* **1997**, *119*, 9175. (b) Templeton, A. C.; Hostetler, M. J.; Kraft, C. T.; Murray, R. W. *J. Am. Chem. Soc.* **1998**, *120*, 1906. (c) Templeton, A. C.; Hostetler, M. J.; Warmoth, E K.; Chen, S.; Hartshorn, C. M.; Krishnamurthy, V. M.; Forbes, M. D. E.; Murray, R. W. *J. Am. Chem. Soc.* **1998**, *120*, 4845.

(20) (a) Hostetler, M. J.; Templeton, A. C.; Murray, R. W. *Langmuir* **1999**, *15*, 3782. (b) Hostetler, M. J.; Green, S. J.; Stokes, J. J.; Murray, R. W. *J. Am. Chem. Soc*. **1996**, *118*, 4212. (c) Hostetler, M. J.; Wingate, J. E.; Zhong, C.-J.; Harris, J. E.; Vachet, R. W.; Clark, M. R.; Londono, J. D.; Green, S. J.; Stokes, J. J.; Wignall, G. D.; Glish, G. L.; Porter, M. D.; Evans, N. D.; Murray, R. W. *Langmuir* **1998**, *14*, 17.

(21) Bibart, R. T.; Vogel, K. W.; Drueckhammer, D. G. *J. Org. Chem*, **1999**, *64*, 2903.

(22) Brust, M.; Walker, M.; Bethell, D.; Schiffrin, D. J.; Whyman, R. *J. Chem. Soc., Chem. Commun.* **1994**, 801.

(23) Runti, C.; Bucher, G. *Ann. Chim. (Rome)* **1957**, *47*, 356.

(24) Ajayan, P. M. *Chem. Rev.* **1999**, *99*, 1787.

(25) Peters, M. J.; McNeil, L. E.; Lu, J. P.; Kahn, D. *Phys. Rev. B* **2000**, *61*, 5939.

(26) Tang, X.-P.; Kleinhammes, A.; Shimoda, H.; Fleming, L.; Bennoune, K. Y.; Sinha, S.; Bower, C.; Zhou, O.; Wu, Y. *Science* **2000**, *288*, 492.